

Fused Dithienogermolodithiophene Low Band Gap Polymers for High-Performance Organic Solar Cells without Processing Additives

Hongliang Zhong,[†] Zhe Li,[†] Florent Deledalle,[†] Elisa Collado Fregoso,[†] Munazza Shahid,[†] Zhuping Fei,[†] Christian B. Nielsen,[†] Nir Yaacobi-Gross,[‡] Stephan Rossbauer,[‡] Thomas D. Anthopoulos,[‡] James R. Durrant,^{*,†} and Martin Heeney^{*,†}

[†]Departments of Chemistry and [‡]Physics, Centre for Plastic Electronics, Imperial College London, London, SW7 2AZ, U.K.

Supporting Information

ABSTRACT: We report the synthesis of a novel ladder-type fused ring donor, dithienogermolodithiophene, in which two thieno[3,2-*b*]thiophene units are held coplanar by a bridging dialkyl germanium. Polymerization of this extended monomer with *N*-octylthienopyrrolodione by Stille polycondensation afforded a polymer, **pDTTG-TPD**, with an optical band gap of 1.75 eV combined with a high ionization potential. Bulk heterojunction solar cells based upon **pDTTG-TPD**:PC₇₁BM blends afforded efficiencies up to 7.2% without the need for thermal annealing or processing additives.

There has been significant recent progress in the development of conjugated polymers for use in organic field effect transistors and bulk heterojunction (BHJ) polymer solar cells.¹ One promising class of polymers for these applications are the so-called ladder polymers,² in which linked aromatic units, such as thiophene or benzene, are forced to be coplanar and fully conjugated by the use of bridging heteroatoms.³ The enforced coplanarity reduces rotational disorder thereby lowering reorganization energy and potentially increasing charge carrier mobility.⁴ The bridging atoms also serve as a point of attachment for the necessary solubilizing groups needed to ensure processable materials.

Within the class of donor–acceptor ladder polymers, bridged bithiophenes have proven to be a particularly useful building block. For example donor–acceptor type copolymers of cyclopentadithiophene (a C bridge) with 2,1,3-benzothiadiazole have exhibited FET mobilities up to 3.3 cm² V^{−1} s^{−1} when substituted with long hexadecyl side chains.⁵ The incorporation of bulky 2-ethylhexyl side chains affords a more amorphous polymer, which nevertheless showing promising BHJ efficiencies of 5.5% when processed from solutions with high-boiling additives.⁶ Changing the bridging heteroatom from C to Si (dithienosilole) or Ge (dithienogermole) for analogous benzothiadiazole copolymers enhances crystallinity, leading to improved charge transport and a reduction in bimolecular recombination.⁷ The improvement in crystallinity has been rationalized on the basis of the longer C–Si/Ge bond compared to the C–C bond, which alters the geometry of the fused heterocycle facilitating enhanced intramolecular interactions.⁸ In addition the replacement of the C bridge with Si or Ge alters the electronic energy levels of the resultant polymers, generally resulting in a lowering of both the HOMO

and LUMO. This has been rationalized by interaction σ^* orbital of the silylene/germylene fragment with the π^* orbital of the aromatic system.⁹

Based upon the promising performance of these bridged dithiophene monomers, we were interested to further extend the conjugation length of the monomer and improve its coplanarity by the incorporation of fused thieno[3,2-*b*]thiophene (TT) instead of thiophene.¹⁰ Thieno[3,2-*b*]thiophene has been widely utilized as a comonomer in a variety of high-performing polymers, where it has been shown to promote intrachain packing and improve charge carrier mobility.¹¹ In addition the incorporation of TT in place of thiophene has been shown to lower the HOMO level (i.e., move further from the vacuum level) of the resultant polymers,^{11a} which is expected to be beneficial for the air stability of both p-type FET polymers and result in an increase in open circuit voltage for photovoltaic donor polymers.

We report the first synthesis of a new donor monomer, in which the bis(thieno[3,2-*b*]thiophene) is bridged by a dialkylgermanium group. The germanium bridging group was utilized because of its improved stability to base over the analogous Si compounds, which facilitates monomer synthesis and purification.^{7d} We chose to copolymerize this novel monomer (DTTG) with *N*-octylthienopyrrolodione (TPD), since the latter has been shown to be a promising comonomer for the donor solar cell polymers.^{12a–d}

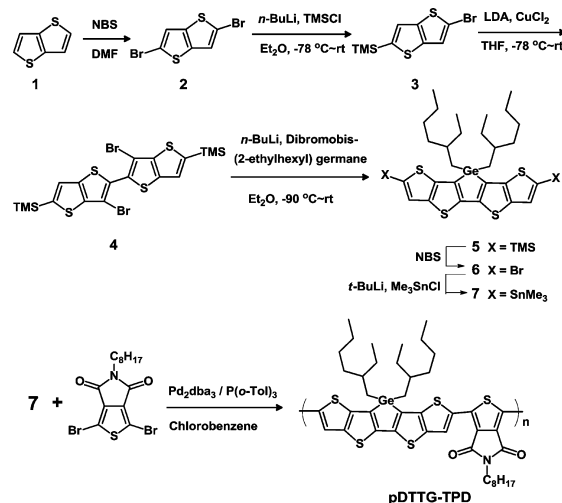
Synthesis of the polymer **pDTTG-TPD** is shown in Scheme 1. Dibromination of commercially available TT with NBS, followed by protection of one of the thienyl bromides as a trimethylsilyl group afforded the previously reported TT derivation 3.¹³ Here we exploit the propensity of thienylhalides to undergo base catalyzed rearrangements (the halogen dance mechanism) to afford the most stable organometallic species.¹⁴ Thus treatment of 5-bromothieno[3,2-*b*]thiophen-2-yl-(trimethyl)silane 3 with 1 equiv of LDA at −78 °C afforded the rearranged 6-bromothieno[3,2-*b*]thiophen-2-yl-(trimethyl)silane. This was not isolated but was oxidatively dimerized *in situ* by treatment with CuCl₂ to afford the dibromide 4 in 70%. This was dilithiated at −90 °C and reacted with dibromobis(2-ethylhexyl) germane to afford the ring-closed germole 5 in 60%. We note that the dianion of 4 had a tendency to decompose by ring opening due to the electron-

Received: November 30, 2012

Published: January 25, 2013



Scheme 1. Synthetic Route to pDTTG-TPD



rich nature of the thieno[3,2-*b*]thiophene. This degradation could be minimized by maintaining the temperature below -90°C and using diethyl ether rather than THF as the solvent.

Conversion of the germole **5** to the required distannyl derivative was achieved by treatment with NBS, followed by lithiation of the resulting dibromide and stannylation at low temperature. Purification was complicated by the tendency to destannylate during attempted chromatographic purification upon silica. Thus preparative recycling GPC was utilized to afford high-purity monomer.

Stille polymerization with TPD was performed under microwave-assisted coupling conditions.¹⁵ The crude polymer was end-capped *in situ* and then purified by precipitation and Soxhlet extraction to afford pDTTG-TPD as a dark solid in 74% yield. The polymer was soluble in chlorobenzene and chloroform upon heating. Molecular weights by GPC in hot chlorobenzene against polystyrene standards were moderate, with a weight average molecular weight (M_w) of 17 KDa and a PDI of 1.4. Here we note that two separate polymerization batches gave very similar results. The thermal stability of the polymer was good, with the onset of degradation occurring at 340°C and 5% weight loss at 385°C (Figure S1). Differential scanning calorimetry (DSC) (Figure S2) showed no obvious thermal transitions between 25 – 300°C .

Optical properties of pDTTG-TPD were characterized by UV/vis absorption spectroscopy. As shown in Figure 1, the solution spectrum displays a maximum at 595 nm and a shoulder at 643 nm. The shoulder is assigned to the aggregation of pDTTG-TPD since heating to 85°C results in a 7 nm blue shift of the maximum and a decline in the relative intensity of the shoulder. This suggests the existence of intermolecular stacking even in dilute solution. Upon film formation the absorption red shifts and the relative peak intensities change, with the former shoulder now becoming the strongest intensity peak at 663 nm with a weaker shoulder at 608 nm. Such changes are indicative of an increasing degree of polymer aggregation and backbone planarization compared to solution. From the onset absorption in the solid state, the optical band gap was calculated to be 1.75 eV.

The tendency to aggregate in the solid state was further investigated by wide-angle X-ray scattering (WAXS). The WAXS patterns of drop cast films before and after annealing at 140°C are shown in Figure S2. Both films displayed a broad

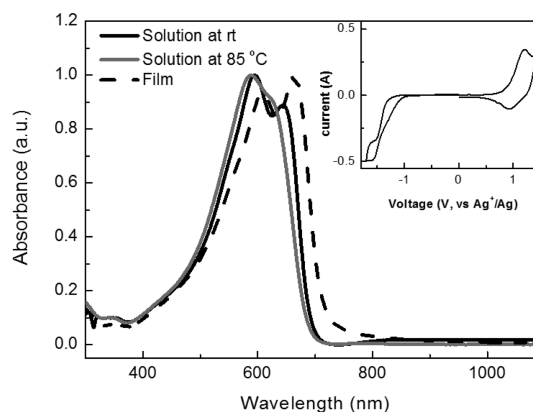


Figure 1. Absorption of pDTTG-TPD in chlorobenzene and as a thin film. Inset: CV of a thin film of pDTTG-TPD in 0.1 M Bu₄NPF₆ acetonitrile solution.

diffraction peak at 24.7° (2θ) corresponding to a *d*-spacing of 3.6 Å, which we attribute to the π – π stacking distance of pDTTG-TPD backbones. This is smaller than the typical distances of 3.7–3.8 Å observed for other TT containing polymers like pBTTT.¹⁶ The as-cast films also show a peak around 4.6° attributable to lamellar packing of the polymer backbones. This lamellar peak increases in intensity upon annealing, suggesting an increase in polymer ordering. These results demonstrate that despite the presence of the two bulky ethyl-hexyl groups on the germanium bridge, the polymer is still able to order in the solid state.

To further investigate the band gap and energy level of pDTTG-TPD, the redox behavior was measured by CV as a thin film. The inserted curve in Figure 1 shows that pDTTG-TPD possesses a reversible oxidation and an irreversible reduction. Based on the assumption that the absolute energy level of ferrocene/ferrocenium (Fc/Fc⁺) is -5.1 eV to vacuum,¹⁷ the energy levels of the HOMO and LUMO were evaluated with the value of -5.68 and -3.88 eV according to their oxidation and reduction onset potentials. As a result the value of electrochemical band gap was calculated as 1.8 eV, which is in excellent agreement with that of optical band gap.

The charge transport behavior of pDTTG-TPD was investigated in bottom contact, bottom gate transistor devices. The dielectric layer (SiO₂) layer was treated with octadecyltrichlorosilane (OTS), and the Au source drain electrodes were treated with pentafluorobenzene thiol before use to afford a reliable work function. Devices were fabricated by spin-coating hot chlorobenzene solutions followed by annealing of the devices at 140°C . The transfer and output characteristics are shown in Figure S3. Some contact resistance is clearly observable in the output plots, most probably due to the mismatch in work function between the low-lying polymer HOMO level and the source electrode. Nevertheless the polymer still exhibited promising p-type transistor performance, with saturated charge carrier mobilities up to $0.11\text{ cm}^2\text{ V}^{-1}\text{ s}^{-1}$ observed.

Photovoltaic performance of pDTTG-TPD was investigated in bulk heterojunction devices with a conventional device configuration of ITO/PEDOT:PSS/PTTGTPD:PC₇₁BM/Ca/Al. Figure 2 shows the best device performance based on the film spin-coated from an optimal 1:2 (w/w) ratio of pDTTG-TPD:PC₇₁BM blend solution in dichlorobenzene at 80°C . Further annealing at 140°C did not change the performance. The optimum active layer thickness was found to be between

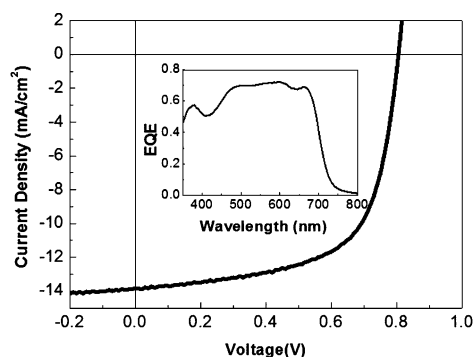


Figure 2. J - V curve of optimized 1:2 pDDTG-TPD:PC₇₁BM blend. Inset: EQE curve for this device.

90–110 nm, limited by the solubility of the donor polymer. The illuminated (AM1.5) current density–voltage (J - V) curve in Figure 2 exhibits a V_{oc} of 0.81 V, a J_{sc} of 13.85 mA cm⁻², and a FF of 64%, leading a PCE of 7.2%. Average device efficiencies were 6.8%. We note that this good performance was achieved without the use of any processing additives. Such additives are often required in the case of largely amorphous donor polymers to drive phase segregation during the film drying process by preferential solubility of one of the components in the additive.¹⁸ In our case, the use of the high boiling additive diiodooctane (DIO) led to deterioration in device performance to 5.9% (Figure S6). To the best of our knowledge pDDTG-TPD is one of the only polymers to exhibit such high efficiencies in a conventional device structure without processing additives.¹⁹

The EQE spectra of the device is displayed in Figure 2 (inset), giving a broad response range covering 350–700 nm. Integration of this spectrum with that of AM1.5 gave 13.80 mA cm⁻², in good agreement with that measured in our solar simulator. Of particular importance is nearly 70% intensity from 500–700 nm, which shows an excellent agreement with the absorption of pDDTG-TPD. In the spectra range from 350–500 nm, there is also average 55% response, assigned to photocurrent generation from PC₇₁BM.

The morphology of the device active layers was characterized by AFM. As shown in Figure S5, the as-cast film exhibits features on the 10–20 nm length scale, suggesting that detrimental large-scale phase segregation is not occurring between the polymer and the PC₇₁BM and that instead the two materials are relatively intimately mixed. Intimate mixing of the donor polymer with PC₇₁BM is supported by PL data, which indicate the PL of the pure polymer film is quenched >96% upon mixing with PC₇₁BM at the 1:2 ratio (Figure S6). We note PC₇₁BM PL was less strongly quenched (~82%), consistent with the lower EQE data obtained following PC₇₁BM excitation and indicative of the formation of relatively pure, aggregated PC₇₁BM domains on length scales comparable to PC₇₁BM exciton diffusion lengths (~5 nm).²⁰

Transient absorption data were employed to assay charge generation and nongeminate recombination in 1:2 pDDTG-TPD:PC₇₁BM blend films. Optical excitation resulted in appearance of a broad transient absorption peak at 1050 nm, typical of polymer positive polarons.²¹ This feature decayed with power law decay dynamics typical of dissociated polarons.²¹ The large amplitude of the transients, even at excitation energy densities as small as 1.3 μJ·cm⁻², suggests that charge generation is very efficient in this system (Figure 3),

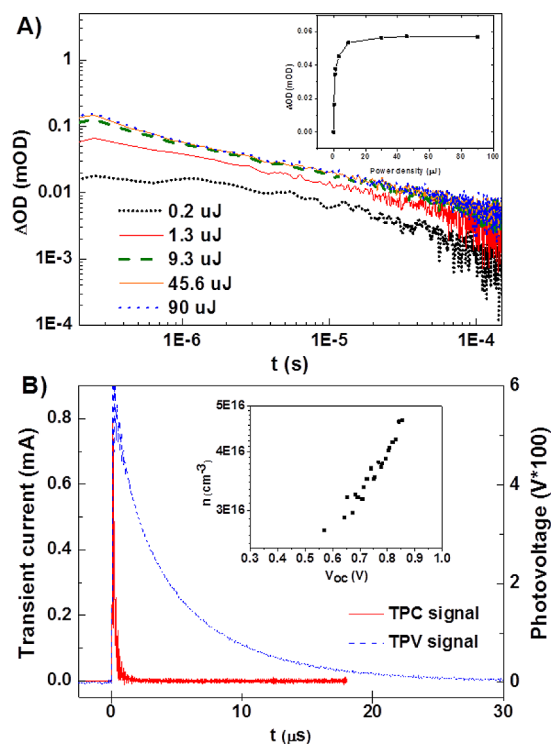


Figure 3. (A) Transient absorption decays of 1:2 pDDTG-TPD:PC₇₁BM blend films as a function of excitation intensity. Inset: Signal amplitude at 250 ns as a function of excitation intensity. (B) Comparison of photocurrent and photovoltage transients of devices under the same background illumination (25% sun). Inset: Charge densities determined from charge extraction data as function of irradiation intensity.

despite the relatively low-energy offset driving charge separation. This ability to separate charge efficiently even with a low-energy offset can most probably be attributed to the donor/acceptor nature of pDDTG-TPD.²² The exponent of the power law decay is ~0.45 and indicative of a reasonably low level of energetic disorder. Similarly, the sharp saturation of the transient signal with increasing excitation density (Figure 3A inset) is indicative of a reasonably low level of intraband trap states, estimated from these data to be $\sim 5 \times 10^{17}$ cm⁻³.

Transient photovoltage, photocurrent, and charge extraction data were further employed to analyze the charge carrier dynamics in 1:2 pDDTG-TPD:PC₇₁BM devices.²³ A comparison of transient photocurrent and photovoltage transients collected under 0.25 sun irradiation indicate rapid charge extraction at short circuit relative to nongeminate recombination at open circuit (decay times of 0.7 and 4 μs respectively, Figure 3B), indicative of efficient charge collection in the device. Charge extraction data (Figure 3B inset) yielded a spatially averaged charge carrier density of 4×10^{16} cm⁻³ under one sun illumination at V_{oc} . The effective transverse drift mobility, determined previously from the charge density at short circuit,²⁴ was found to be of 1.4×10^{-4} cm² V⁻¹ s⁻¹. Open circuit voltages calculated from these charge densities and decay times are in excellent agreement with directly measured values (Figure S7), indicating that V_{oc} is determined by nongeminate recombination.

For most recently reported donor–acceptor polymers, increases in polymer ionization potential relative to P3HT controls are only partially reflected in increases in V_{oc} .^{19,21} In contrast our analysis of $n(V_{oc})$ from charge extraction data

indicates the larger electronic band gap of the pDTTG-TPD blend devices results quantitatively in an increase in V_{oc} specifically a measured increase of electronic band gap by 247 mV relative to P3HT agrees quantitatively with an increase in V_{oc} by ~ 250 mV.²⁵ Indeed the mobility and recombination data observed here for pDTTG-TPD are very similar to P3HT:PCBM devices, indicating comparable 'reduced Langevin' recombination (Langevin prefactor of $\sim 10^{-3}$).²⁰ This is indicative of a favorable film microstructure for charge collection. These favorable charge carrier dynamics, combined with an increased electronic bandgap without loss of charge photogeneration efficiency, can explain the high efficiency of the pDTTG-TPD devices reported herein.

In conclusion, we synthesized a novel ladder-type fused ring donor DTTG incorporating two thieno[3,2-*b*]thiophene units bridged by a dialkylgermanium. Copolymerization with *N*-octylthienopyrrolodione by Stille polycondensation affords a polymer with a low optical band gap combined with a high ionization potential. Photovoltaic devices based upon pDTTG-TPD:PC₇₁BM blends exhibit efficiencies up to 7.2% for as-cast films with no processing additives or thermal annealing. These preliminary results indicate that polymers containing fused DTTG moieties are promising candidates for high-efficiency OPV devices. We note the synthetic route outlined here enables considerable synthetic scope to further tune the performance by modification of the bridging heteroatom.

■ ASSOCIATED CONTENT

■ Supporting Information

Experimental details and characterization data. This material is available free of charge via the Internet at <http://pubs.acs.org>.

■ AUTHOR INFORMATION

Corresponding Author

j.durrant@imperial.ac.uk; m.heeney@imperial.ac.uk

Notes

The authors declare no competing financial interest.

■ ACKNOWLEDGMENTS

This work was supported by EU grant 287818 (X10D) and EPSRC grant EP/H040218/1 APEX and a Samsung GRO grant.

■ REFERENCES

- (1) (a) Duan, C.; Huang, F.; Cao, Y. *J. Mater. Chem.* **2012**, *22*, 10416.
- (2) Chochos, C. L.; Choulis, S. A. *Prog. Polym. Sci.* **2011**, *36*, 1326.
- (3) Scherf, U. *J. Mater. Chem.* **1999**, *9*, 1853.
- (4) Xie, L.-H.; Yin, C.-R.; Lai, W.-Y.; Fan, Q.-L.; Huang, W. *Prog. Polym. Sci.* **2012**, *37*, 1192.
- (5) McCulloch, I.; Ashraf, R. S.; Biniek, L.; Bronstein, H.; Combe, C.; Donaghey, J. E.; James, D. I.; Nielsen, C. B.; Schroeder, B. C.; Zhang, W. M. *Acc. Chem. Res.* **2012**, *45*, 714.
- (6) Tsao, H. N.; Cho, D. M.; Park, I.; Hansen, M. R.; Mavrinskiy, A.; Yoon, D. Y.; Graf, R.; Pisula, W.; Spiess, H. W.; Muellen, K. *J. Am. Chem. Soc.* **2011**, *133*, 2605.
- (7) (a) Muehlbacher, D.; Scharber, M.; Morana, M.; Zhu, Z.; Waller, D.; Gaudiana, R.; Brabec, C. *Adv. Mater.* **2006**, *18*, 2884. (b) Peet, J.; Kim, J. Y.; Coates, N. E.; Ma, W. L.; Moses, D.; Heeger, A. J.; Bazan, G. C. *Nat. Mater.* **2007**, *6*, 497.
- (8) (a) Hou, J. H.; Chen, H. Y.; Zhang, S. Q.; Li, G.; Yang, Y. *J. Am. Chem. Soc.* **2008**, *130*, 16144. (b) Ohshita, J.; Hwang, Y. M.; Mizumo, T.; Yoshida, H.; Ooyama, Y.; Harima, Y.; Kunugi, Y. *Organometallics* **2011**, *30*, 3233. (c) Gendron, D.; Morin, P.-O.; Berrouard, P.; Allard, N.; Aïch, B. R.; Garon, C. N.; Tao, Y.; Leclerc, M. *Macromolecules* **2011**, *44*, 7188. (d) Fei, Z.; K, J. S.; Smith, J.; Buchaca Domingo, E.; Anthopoulos, T. D.; Stingelin, N.; Watkins, S.; Kim, J.-S.; Heeney, M. *J. Mater. Chem.* **2011**, *21*, 16257.
- (9) (a) Chen, H. Y.; Hou, J. H.; Hayden, A. E.; Yang, H.; Houk, K. N.; Yang, Y. *Adv. Mater.* **2010**, *22*, 371. (b) Scharber, M. C.; Koppe, M.; Gao, J.; Cordella, F.; Loi, M. A.; Denk, P.; Morana, M.; Egelhaaf, H. J.; Forberich, K.; Dennler, G.; Gaudiana, R.; Waller, D.; Zhu, Z. G.; Shi, X. B.; Brabec, C. J. *Adv. Mater.* **2010**, *22*, 367. (c) Amb, C. M.; Chen, S.; Graham, K. R.; Subbiah, J.; Small, C. E.; So, F.; Reynolds, J. R. *J. Am. Chem. Soc.* **2011**, *133*, 10062.
- (10) (a) Ohshita, J. *Macromol. Chem. Phys.* **2009**, *210*, 1360. (b) Yamaguchi, S.; Tamao, K. *J. Chem. Soc., Dalton Trans.* **1998**, *0*, 3693.
- (11) (a) Wan, J.-H.; Fang, W.-F.; Li, Z.-F.; Xiao, X.-Q.; Xu, Z.; Deng, Y.; Zhang, L.-H.; Jiang, J.-X.; Qiu, H.-Y.; Wu, L.-B.; Lai, G.-Q. *Chem. Asian J.* **2010**, *5*, 2290.
- (12) (a) McCulloch, I.; Heeney, M.; Chabinyc, M. L.; DeLongchamp, D.; Kline, R. J.; Coelle, M.; Duffy, W.; Fischer, D.; Gundlach, D.; Hamadani, B.; Hamilton, R.; Richter, L.; Salles, A.; Shkunov, M.; Sparrowe, D.; Tierney, S.; Zhang, W. *Adv. Mater.* **2009**, *21*, 1091. (b) Li, Y. N.; Singh, S. P.; Sonar, P. *Adv. Mater.* **2010**, *22*, 4862. (c) Gao, P.; Cho, D.; Yang, X.; Enkelmann, V.; Baumgarten, M.; Müllen, K. *Chem.—Eur. J.* **2010**, *16*, 5119.
- (13) (a) Chu, T.-Y.; Lu, J.; Beaupré, S.; Zhang, Y.; Pouliot, J.-R. m.; Wakim, S.; Zhou, J.; Leclerc, M.; Li, Z.; Ding, J.; Tao, Y. *J. Am. Chem. Soc.* **2011**, *133*, 4250. (b) Guo, X.; Xin, H.; Kim, F. S.; Liyanage, A. D. T.; Jenekhe, S. A.; Watson, M. D. *Macromolecules* **2010**, *44*, 269. (c) Li, Z.; Tsang, S.-W.; Du, X.; Scoles, L.; Robertson, G.; Zhang, Y.; Toll, F.; Tao, Y.; Lu, J.; Ding, J. *Adv. Funct. Mater.* **2011**, *21*, 3331. (d) Piliago, C.; Holcombe, T. W.; Douglas, J. D.; Woo, C. H.; Beaujuge, P. M.; Fréchet, J. M. J. *J. Am. Chem. Soc.* **2010**, *132*, 7595.
- (14) Miguel, L. S.; Matzger, A. J. *J. Org. Chem.* **2008**, *73*, 7882.
- (15) (a) Getmanenko, Y. A.; Tongwa, P.; Timofeeva, T. V.; Marder, S. R. *Org. Lett.* **2010**, *12*, 2136. (b) Al-Hashimi, M.; Labram, J. G.; Watkins, S.; Motevalli, M.; Anthopoulos, T. D.; Heeney, M. *Org. Lett.* **2010**, *12*, 5478.
- (16) Tierney, S.; Heeney, M.; McCulloch, I. *Synth. Met.* **2005**, *148*, 195.
- (17) Chabinyc, M. L.; Toney, M. F.; Kline, R. J.; McCulloch, I.; Heeney, M. *J. Am. Chem. Soc.* **2007**, *129*, 3226.
- (18) Cardona, C. M.; Li, W.; Kaifer, A. E.; Stockdale, D.; Bazan, G. C. *Adv. Mater.* **2011**, *23*, 2367.
- (19) Lee, J. K.; Ma, W. L.; Brabec, C. J.; Yuen, J.; Moon, J. S.; Kim, J. Y.; Lee, K.; Bazan, G. C.; Heeger, A. J. *J. Am. Chem. Soc.* **2008**, *130*, 3619.
- (20) (a) Bartelt, J. A.; Beiley, Z. M.; Hoke, E. T.; Mateker, W. R.; Douglas, J. D.; Collins, B. A.; Graham, K. R.; Amassian, A.; Ade, H.; Fréchet, J. M. J.; Toney, M. F.; McGehee, M. D. *Adv. Energy Mater.* doi:10.1002/aenm.201200637; (b) Hoke, E. T.; Vandewal, K.; Bartelt, J. A.; Mateker, W. R.; Douglas, J. D.; Noriega, R.; Graham, K. R.; Fréchet, J. M. J.; Salles, A.; McGehee, M. D. *Adv. Energy Mater.* **2012**, DOI: 10.1002/aenm.201200474. (c) Dou, L.; Chang, W.-H.; Gao, J.; Chen, C.-C.; You, J.; Yang, Y. *Adv. Mater.* **2012**, DOI: 10.1002/adma.201203827.
- (21) Dimitrov, S. D.; Nielsen, C. B.; Shoaee, S.; Shukya Tuladhar, P.; Du, J.; McCulloch, I.; Durrant, J. R. *J. Phys. Chem. Lett.* **2011**, *3*, 140.
- (22) Clarke, T. M.; Jamieson, F. C.; Durrant, J. R. *J. Phys. Chem. C* **2009**, *113*, 20934.
- (23) Clarke, T.; Ballantyne, A.; Jamieson, F.; Brabec, C.; Nelson, J.; Durrant, J. *Chem. Commun.* **2009**, 89.
- (24) Credginton, D.; Durrant, J. R. *J. Phys. Chem. Lett.* **2012**, *3*, 1465.
- (25) Shuttle, C. G.; Hamilton, R.; Nelson, J.; O'Regan, B. C.; Durrant, J. R. *Adv. Funct. Mater.* **2010**, *20*, 698.
- (26) Maurano, A.; Shuttle, C. C.; Hamilton, R.; Ballantyne, A. M.; Nelson, J.; Zhang, W. M.; Heeney, M.; Durrant, J. R. *J. Phys. Chem. C* **2011**, *115*, 5947.